J. Fluid Mech. (1972), *vol.* 54, *part* 1, *pp.* 49–61
Printed in Great Britain

Rotation of a cylinder about an eccentric parallel axis in a viscous fluid

By CHANG-YI WANG

Department of Mathematics, Michigan State University, East Lansing

(Received 20 June 1971 and in revised form 22 November 1971)

A circular cylinder in an infinite fluid rotates rigidly about a fixed axis which is parallel to, but does not coincide with, its geometric axis. It is found that, depending on the relative magnitude of the Reynolds number R and eccentricity ϵ, the flow may have two, one or no boundary layers. General solutions for $R \ll \epsilon^{-\frac{3}{2}}$ are obtained. It is found that owing to eccentricity there exist both a flow periodic in the circumferential direction and a non-periodic flow which is a function only of the radial distance from the centre of the cylinder. The non-periodic flow is caused by the nonlinear Reynolds stress and contributes to the torque experienced by the cylinder. The high Reynolds number case,

$$1 \ll R \ll \epsilon^{-\frac{3}{2}},$$

is solved by matched asymptotic expansions. The stream function can be represented by Hankel functions of order $\frac{1}{3}$, and a slight *decrease* in torque is found. In the low Reynolds number case, $R \ll 1$, the torque is increased owing to eccentricity when $R < 0{\cdot}145$ and decreased when $R > 0{\cdot}145$. A physical explanation is presented.

1. Introduction

Rotating circular cylinders or shafts immersed in viscous fluids play an important role in many engineering devices. Often the rotation axis is parallel to but may not coincide with the geometric axis of the cylinder, owing either to imprecise machining, to worn out bearing supports, or to elastic instability caused by centrifugal forces. Although the eccentricity, i.e. the distance between the two axes divided by cylinder radius, is usually small, it does perturb the surrounding fluid. This paper investigates the perturbed flow field and the additional torque and forces caused by eccentricity.

Let us consider a cylinder of radius a which is rotating counter-clockwise with angular velocity ω about the rotation axis B in a viscous fluid (figure 1). The distance between the rotation axis B and the geometric axis O is ϵa, where ϵ, the eccentricity, is small compared to unity. We then normalize all lengths by a, velocities by ωa, and the time by $1/\omega$.

Now the boundary conditions are difficult to apply in the inertial frame x', y' whose origin lies on the fixed point at B. These conditions are simplified if we

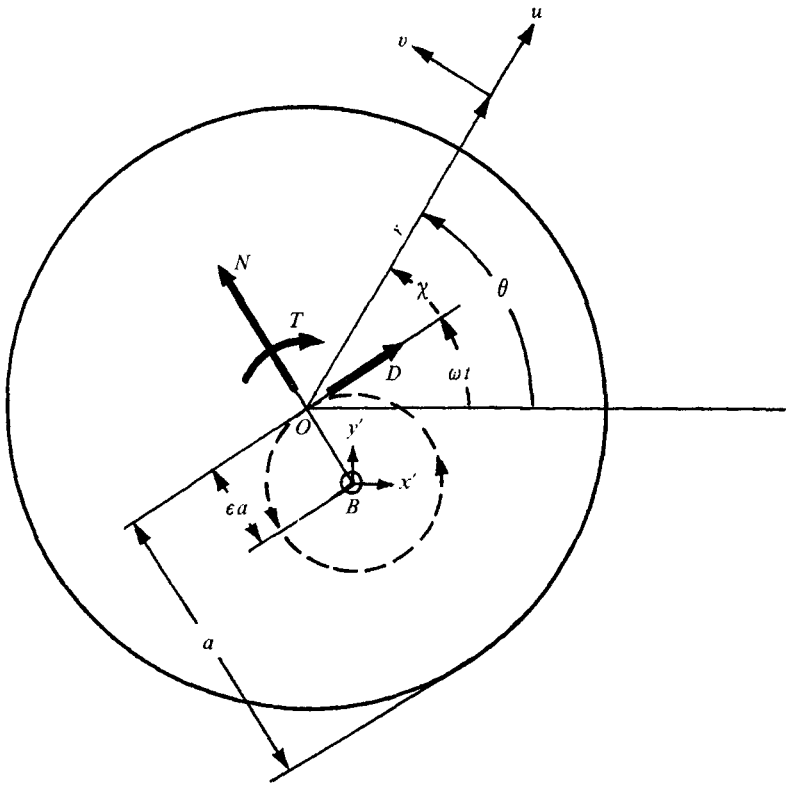

FIGURE 1. The co-ordinate system and nomenclature.
N = normal force, D = drag, T = torque.

consider a translational frame x, y (or r, θ, in polar co-ordinates) attached to the moving point at O. The relationship between these co-ordinates is

$$r\cos\theta \equiv x = x' + \epsilon\sin t, \tag{1.1}$$

$$r\sin\theta \equiv y = y' - \epsilon\cos t. \tag{1.2}$$

Let u and v be the velocity components relative to the translating frame in the directions of r and θ respectively. These velocities differ from the corresponding velocities in the inertial frame (u', v') by a uniform translational motion:

$$u - u' = \epsilon\cos(\theta - t), \tag{1.3}$$

$$v - v' = -\epsilon\sin(\theta - t). \tag{1.4}$$

The boundary conditions become

$$u = 0, \quad v = 1 \quad \text{on} \quad r = 1, \tag{1.5}$$

$$u \to \epsilon\cos(\theta - t), \quad v \to -\epsilon\sin(\theta - t) \quad \text{as} \quad r \to \infty. \tag{1.6}$$

The governing Navier–Stokes equation then becomes

$$\frac{\partial}{\partial t}\nabla^2\Psi - \frac{1}{r}\frac{\partial(\Psi, \nabla^2\Psi)}{\partial(r, \theta)} = \frac{1}{R}\nabla^4\Psi, \tag{1.7}$$

where $\Psi = \int ru\,d\theta = -\int v\,dr$ is the stream function and $R = \omega a^2/\nu$ is the Reynolds

number. Owing to symmetry we can see at once that the stream function Ψ' depends on only *two* variables, r and χ, where $\chi = \theta - t$. Thus

$$-\frac{\partial}{\partial \chi}\nabla^2\Psi' - \frac{1}{r}\frac{\partial(\Psi', \nabla^2\Psi')}{\partial(r,\chi)} = \frac{1}{R}\nabla^4\Psi', \tag{1.8}$$

where $$\nabla^2 = \frac{\partial^2}{\partial r^2} + \frac{1}{r}\frac{\partial}{\partial r} + \frac{1}{r^2}\frac{\partial^2}{\partial \chi^2},$$

and the boundary conditions are

$$\Psi' = 0, \quad \partial\Psi'/\partial r = -1 \quad \text{on} \quad r = 1, \tag{1.9}$$

$$\Psi' \to \epsilon r \sin\chi \quad \text{as} \quad r \to \infty. \tag{1.10}$$

The boundary conditions suggest that we also *deduct* the primary flow, an irrotational vortex, from our solution. We set

$$\Psi' = -\ln r + \epsilon\psi(r,\chi), \tag{1.11}$$

where $\epsilon\psi$ represents the perturbation due to eccentricity. The problem then becomes

$$\left(\frac{1}{r^2} - 1\right)\frac{\partial}{\partial \chi}\nabla^2\psi - \frac{\epsilon}{r}\frac{\partial(\psi, \nabla^2\psi)}{\partial(r,\chi)} = \frac{1}{R}\nabla^4\psi, \tag{1.12}$$

with the boundary conditions

$$\psi = 0, \quad \partial\psi/\partial r = 0 \quad \text{on} \quad r = 1, \tag{1.13}$$

$$\psi \to r\sin\chi \quad \text{as} \quad r \to \infty. \tag{1.14}$$

2. Simplifications of the governing equation

In the (r,χ) co-ordinates the flow is steady and boundary conditions (1.13) and (1.14) suggest a uniform flow past a circular cylinder. The governing equation (1.12), however, is quite different from the usual form of the Navier–Stokes equations. Many different simplifications can be made depending on the magnitude of the Reynolds number. For large Reynolds numbers, we take

$$R = \alpha/\epsilon^\gamma, \quad r = 1 + \epsilon^\beta\eta,$$

where α, β, and γ are constants of order unity and η is a stretched variable. The orders of magnitude of the separate terms in (1.12) become $\epsilon^{-\beta}$, $\epsilon^{1-3\beta}$, and $\epsilon^{\gamma-4\beta}$ respectively. We see that the nonlinear terms are important only when

$$1 - 3\beta \leqslant \gamma - 4\beta \quad \textit{and} \quad 1 - 3\beta \leqslant -\beta.$$

Therefore the nonlinear terms can be important only in a boundary-layer region of order $\epsilon^{\frac{1}{2}}$ when also R is of order $\epsilon^{-\frac{3}{2}}$ or larger. The flow is primarily linear when $R \ll \epsilon^{-\frac{3}{2}}$.

As the Reynolds number varies from inifinity to zero, the parameter γ changes from $+\infty$ to $-\infty$. A careful study of the relative magnitudes of the terms in (1.12) yields the five cases given below, which are distinguished through the five different simplifications of the governing equation as γ is varied. In cases 1, 2 and 3 equation (1.12) presents singular perturbation problems. In these cases the radial co-ordinate r has to be stretched, indicating the existence of boundary layers near the cylinder.

Case 1: $\infty > \gamma > \frac{3}{2}$. Two co-existing boundary layers of order $\epsilon^{\gamma-1}$ and $\epsilon^{\frac{1}{2}}$ exist. The leading terms give

$$-\partial(\psi, \psi_{\eta\eta})/\partial(\eta, \chi) = (1/\alpha)\psi_{\eta\eta\eta\eta} \quad \text{for} \quad \beta \geqslant \gamma - 1, \tag{2.1}$$

$$-2\eta\psi_{\chi\eta\eta} - \partial(\psi, \psi_{\eta\eta})/\partial(\eta, \chi) = 0 \quad \text{for} \quad \gamma - 1 > \beta \geqslant \tfrac{1}{2}, \tag{2.2}$$

$$\partial(\nabla^2\psi)/\partial\chi = 0 \quad \text{for} \quad \beta < \tfrac{1}{2}. \tag{2.3}$$

Case 2: $\gamma = \frac{3}{2}$. There exists one boundary layer of order $\epsilon^{\frac{1}{3}}$.

$$-2\eta\psi_{\chi\eta\eta} - \partial(\psi, \psi_{\eta\eta})/\partial(\eta, \chi) = (1/\alpha)\psi_{\eta\eta\eta\eta} \quad \text{for} \quad \beta \geqslant \tfrac{1}{2}, \tag{2.4}$$

$$\partial(\nabla^2\psi)/\partial\chi = 0 \quad \text{for} \quad \beta < \tfrac{1}{2}. \tag{2.5}$$

Case 3: $\frac{3}{2} > \gamma > 0$. There exists one boundary layer of order $\epsilon^{\frac{1}{3}\gamma}$.

$$-2\eta\psi_{\chi\eta\eta} = (1/\alpha)\psi_{\eta\eta\eta\eta} \quad \text{for} \quad \beta \geqslant \tfrac{1}{3}\gamma, \tag{2.6}$$

$$\partial(\nabla^2\psi)/\partial\chi = 0 \quad \text{for} \quad \beta < \tfrac{1}{3}\gamma. \tag{2.7}$$

Case 4: $\gamma = 0$. There are no boundary layers for any value of β.

$$\left(\frac{1}{r^2} - 1\right)\frac{\partial}{\partial\chi}\nabla^2\psi = \frac{1}{\alpha}\nabla^4\psi \equiv \frac{1}{R}\nabla^4\psi. \tag{2.8}$$

Case 5: $0 > \gamma > -\infty$. There are no boundary layers for any value of β.

$$-\frac{\partial}{\partial\chi}\nabla^2\psi = \frac{1}{\alpha\epsilon^{|\gamma|}}\nabla^4\psi \equiv \frac{1}{R}\nabla^4\psi. \tag{2.9}$$

For low Reynolds numbers, the Stokes solution of $\nabla^4\psi = 0$ fails at a distance of $r \approx \epsilon^{-\frac{1}{3}|\gamma|}$, which is the well-known 'Stokes paradox'. Equation (2.9) represents the governing equation for $r \geqslant \epsilon^{-\frac{1}{3}|\gamma|}$. Since it also includes the Stokes solution $\nabla^4\psi = 0$, we shall use it for the entire range of r.

In the remainder of this paper we study in detail cases 3, 4 and 5, for which the nonlinearities do not enter the zeroth-order perturbations.

3. General considerations for $R \ll \epsilon^{-\frac{3}{2}}$

Let us separate the stream function into a periodic part denoted by $\tilde{\psi}(r, \chi)$ and a non-periodic part denoted by $\overline{\psi}(r)$:

$$\psi = \tilde{\psi}(r, \chi) + \overline{\psi}(r), \tag{3.1}$$

where $\overline{\psi}(r)$ is given by the average

$$\overline{\psi}(r) = \frac{1}{2\pi}\int_0^{2\pi} \psi(r, \chi)\, d\chi. \tag{3.2}$$

Then (1.12) becomes

$$\left(\frac{1}{r^2} - 1\right)\frac{\partial}{\partial\chi}\nabla^2\tilde{\psi} - \frac{\epsilon}{r}\left\{\frac{\partial(\tilde{\psi}, \nabla^2\tilde{\psi})}{\partial(r, \chi)}\right\} - \frac{\epsilon}{r}\left[\frac{\partial(\tilde{\psi}, \nabla^2\overline{\psi})}{\partial(r, \chi)} + \frac{\partial(\overline{\psi}, \nabla^2\tilde{\psi})}{\partial(r, \chi)}\right] = \frac{1}{R}\nabla^4\tilde{\psi}, \tag{3.3}$$

$$-\frac{\epsilon}{r}\left[\overline{\frac{\partial(\tilde{\psi}, \nabla^2\tilde{\psi})}{\partial(r, \chi)}}\right] = \frac{1}{R}\nabla^4\overline{\psi}, \tag{3.4}$$

where $\{\,\}$ and $[\bar{}]$ denote the periodic and non-periodic parts of the product respectively.

From the discussion in § 2, if $R = \alpha\epsilon^{-\gamma}$, where α is a constant of order unity and $-\infty < \gamma < \frac{3}{2}$, the nonlinear terms in (3.3) could never become important at any radius r. Hence the leading terms are

$$\left(\frac{1}{r^2}-1\right)\frac{\partial}{\partial\chi}\nabla^2\tilde{\psi} = \frac{1}{R}\nabla^4\tilde{\psi}. \tag{3.5}$$

The solution of (3.5) together with the boundary conditions $\tilde{\psi}(1,\chi) = 0$, $\partial\tilde{\psi}(1,\chi)/\partial r = 0$ and $\tilde{\psi}(\infty,\chi)\to -ire^{i\chi}$ is

$$\tilde{\psi}(r,\chi) = \frac{-ie^{i\chi}}{\int_1^\infty H_\kappa^{(1)}[(iR)^{\frac{1}{2}}r]\,dr}\left[r\int_1^r H_\kappa^{(1)}[(iR)^{\frac{1}{2}}r]\,dr - \frac{1}{r}\int_1^r r^2 H_\kappa^{(1)}[(iR)^{\frac{1}{2}}r]\,dr\right], \tag{3.6}$$

where $\kappa = (1+iR)^{\frac{1}{2}}$ and $H_\kappa^{(1)}$ is the Hankel function of the first kind with complex argument and complex order. The non-periodic solution is then obtained from (3.4):

$$\nabla^4\overline{\psi}(r) = 4B(r), \tag{3.7}$$

where

$$B(r) = -\frac{\epsilon R}{4r}\left[\overline{\frac{\partial(\tilde{\psi},\nabla^2\tilde{\psi})}{\partial(r,\chi)}}\right] = -\frac{\epsilon R}{8r}\left[\frac{\partial(\tilde{\psi}^*,\nabla^2\tilde{\psi})}{\partial(r,\chi)}\right], \tag{3.8}$$

$\tilde{\psi}^*$ being the complex conjugate of $\tilde{\psi}$. The solution to (3.7) is

$$\begin{aligned}\overline{\psi}(r) = {} & \int_1^r Br^3(1-\ln r)\,dr - \int_1^\infty Br(1+\ln r)\,dr + \ln r\left[\int_1^r Br^3\,dr - \int_1^\infty Br(1+2\ln r)\,dr\right] \\ & + r^2\left[-\int_1^r Br(1+\ln r)\,dr + \int_1^\infty Br(1+\ln r)\,dr\right] + r^2\ln r\left[\int_1^r Br\,dr - \int_1^\infty Br\,dr\right],\end{aligned} \tag{3.9}$$

where we have made use of the boundary conditions that the velocities be zero on $r = 1$ and as $r\to\infty$.

The periodic flow (3.6) creates pressure and shear-stress distributions on the cylinder. Substitution into the Navier–Stokes equation for the θ velocity component yields

$$\frac{\tilde{p}}{\rho\omega^2a^2\epsilon} = \frac{i}{R}\frac{\partial}{\partial r}(\nabla^2\tilde{\psi})_{r=1} = \frac{(iR)^{\frac{1}{2}}e^{i\chi}}{R\int_1^\infty H_\kappa^{(1)}[(iR)^{\frac{1}{2}}r]\,dr}[H_{\kappa-1}^{(1)}[(iR)^{\frac{1}{2}}] - H_{\kappa+1}^{(1)}[(iR)^{\frac{1}{2}}]], \tag{3.10}$$

$$\frac{\tilde{\tau}}{\mu\omega\epsilon} = -\frac{\partial^2\tilde{\psi}}{\partial r^2}\bigg|_{r=1} = \frac{2ie^{i\chi}}{\int_1^\infty H_\kappa^{(1)}[(iR)^{\frac{1}{2}}r]\,dr}H_\kappa^{(1)}[(iR)^{\frac{1}{2}}], \tag{3.11}$$

where a tilde indicates 'the periodic part'. If the normal force N, the drag D and the torque T are in the directions shown in figure 1, then the forces due to the periodic flow $\tilde{\psi}$ are

$$N = a\int_0^{2\pi}(\tilde{\tau}\cos\chi - \tilde{p}\sin\chi)\,d\chi, \tag{3.12}$$

$$D = a\int_0^{2\pi}(-\tilde{\tau}\sin\chi - \tilde{p}\cos\chi)\,d\chi. \tag{3.13}$$

The normal force does not contribute to the torque but the drag force yields a torque

$$T = \epsilon a^2 \int_0^{2\pi} (-\tilde{\tau}\sin\chi - \tilde{p}\cos\chi)\, d\chi. \tag{3.14}$$

The non-periodic flow $\bar{\psi}(r)$ gives no force but yields a torque

$$T' = 2\pi a^2 \mu\omega\epsilon \frac{d^2\bar{\psi}}{dr^2}\bigg|_{r=1} = 8\pi a^2\mu\omega\epsilon \int_1^\infty Br\ln r\, dr. \tag{3.15}$$

If the Reynolds number R is of order unity, then $\tilde{p}$, $\tilde{\tau}$ and B are of order ϵ and both T and T' are of order ϵ^2. We see that the linear secondary flow $\tilde{\psi}$ and the nonlinear secondary flow $\bar{\psi}$ contribute equally to the additional torque experienced. The total torque is the sum of the torque due to the irrotational vortex $\ln r$ in (1.11) and the additional torque due to secondary flows:

$$T_{\text{total}} = 2\pi a^2\mu\omega + T + T'. \tag{3.16}$$

Very little physical insight can be obtained from the general solutions (3.6) and (3.9) because these involve integration of complicated Hankel functions. In what follows we study cases 3 and 5, for which the solution becomes simpler, at the expense of applicability in a more restricted range of Reynolds numbers.

4. High Reynolds numbers $1 \ll R \ll \epsilon^{-\frac{3}{2}}$

Since the leading terms of the governing equation retain the same form for this range of Reynolds numbers we can take $R = \alpha/\epsilon$ to represent this regime, without loss of generality. According to the discussion in § 2 there exists a boundary layer of $O(\epsilon^{\frac{1}{2}})$ near the cylinder. We now use the method of inner and outer expansions, which is much simpler than taking the proper limits of (3.6) and (3.9).

From (2.7) the outer flow is potential since it is irrotational at infinity. The solution is thus

$$\tilde{\psi}_0 = -i(r - 1/r)\, e^{i\chi}. \tag{4.1}$$

Inside the boundary layer we set $r = 1 + \epsilon^{\frac{1}{2}}\eta$ and $\tilde{\psi} = \epsilon^{\frac{1}{2}}\tilde{\psi}_i$, so that the governing equation is

$$-2\eta \frac{\partial^3\tilde{\psi}_i}{\partial\chi\partial\eta^2} = \frac{1}{\alpha}\frac{\partial^4\tilde{\psi}_i}{\partial\eta^4}, \tag{4.2}$$

or

$$f^{\text{iv}}(\eta) + 2\alpha\eta i f'' = 0, \tag{4.3}$$

where $\tilde{\psi}_i = f(\eta)\, e^{i\chi}$. The solution which matches the outer flow (4.1) at infinity and has zero velocity on the boundary is

$$f(\eta) = 3^{\frac{1}{2}} i^{-\frac{1}{6}} \eta F(\tfrac{2}{3} 2^{\frac{1}{2}} \alpha^{\frac{1}{2}} \eta^{\frac{3}{2}}) + 3^{\frac{1}{2}} i^{\frac{2}{3}} \eta G(\tfrac{2}{3} 2^{\frac{1}{2}} \alpha^{\frac{1}{2}} \eta^{\frac{3}{2}}) + \Gamma(\tfrac{2}{3}) 3^{\frac{7}{6}} i^{\frac{1}{3}}/\pi(2\alpha)^{\frac{1}{3}}, \tag{4.4}$$

where

$$F(\lambda) = \int_0^\lambda H^{(1)}_{\frac{1}{3}}(i^{\frac{1}{2}}\lambda)\, d\lambda, \tag{4.5}$$

$$G(\lambda) = H^{(1)}_{\frac{2}{3}}(i^{\frac{1}{2}}\lambda). \tag{4.6}$$

To the author's knowledge, there are only two tabulations of Hankel functions of order $\frac{1}{3}$. General complex arguments have been tabulated by the Harvard Computation Laboratory (1945), but this source is very inconvenient to use for

an argument of $i^{\frac{1}{2}}\lambda$. The other tabulation is due to Chang (1948), in connexion with the elastic deformation of toroidal shells. Chang's tables of $H_{\frac{1}{3}}^{(1)}(i^{\frac{1}{2}}\lambda)$ have numerous errors, however. A more refined set of values of $H_{\frac{1}{3}}^{(1)}(i^{\frac{1}{2}}\lambda)$ together with $H_{\frac{2}{3}}^{(1)}(i^{\frac{1}{2}}\lambda)$, correct to six significant figures, is presented in table 1. The integral $\int_\lambda^\infty H_{\frac{1}{3}}^{(1)}(i^{\frac{1}{2}}\lambda)\,d\lambda$ is tabulated in table 2. The Hankel functions were calculated by means of computer program NBS HF13 for general complex arguments supplied by the U.S. Department of Commerce. The series representation is used for small arguments and the asymptotic form is used for large arguments. The integral of $H_{\frac{1}{3}}^{(1)}$ is obtained by Simpson's rule with the error estimated by varying the range and mesh size of numerical integration. Since

$$F(\infty) = \int_0^\infty H_{\frac{1}{3}}^{(1)}(i^{\frac{1}{2}}\lambda)d\lambda = (2/3^{\frac{1}{2}})\,i^{-\frac{5}{6}} = 0{\cdot}298858 - 1{\cdot}115355i, \tag{4.7}$$

$F(\lambda)$ can be easily obtained from the table by subtraction.

The boundary-layer flow $\tilde{\psi}_i$ in turn creates a higher order outer flow:

$$\tilde{\psi}_1 = \frac{\Gamma(\frac{2}{3})3^{\frac{7}{6}}i^{\frac{4}{3}}}{\pi(2\alpha)^{\frac{1}{3}}}\frac{e^{i\chi}}{r}. \tag{4.8}$$

A uniformly valid composite solution for the periodic stream function can also be constructed:

$$\begin{aligned}\tilde{\psi}(r,\chi) = {} & -i\left(r-\frac{1}{r}\right)e^{i\chi} + \epsilon^{\frac{1}{3}}\left[\frac{\Gamma(\frac{2}{3})\,3^{\frac{7}{6}}i^{\frac{4}{3}}}{\pi(2\alpha)^{\frac{1}{3}}}\right]\frac{e^{i\chi}}{r} \\ & + \epsilon^{\frac{1}{3}}[3^{\frac{1}{2}}i^{-\frac{1}{6}}\eta F(\tfrac{2}{3}2^{\frac{1}{2}}\alpha^{\frac{1}{2}}\eta^{\frac{3}{2}}) + 3^{\frac{1}{2}}i^{\frac{2}{3}}\eta G(\tfrac{2}{3}2^{\frac{1}{2}}\alpha^{\frac{1}{2}}\eta^{\frac{3}{2}})] + O(\epsilon^{\frac{2}{3}}).\end{aligned} \tag{4.9}$$

Outside the boundary layer of $O(\epsilon^{\frac{1}{3}})$ the vorticity $\nabla^2\tilde{\psi}$, and thus the driving term of (3.4), decay exponentially to zero. To balance this, the order of the non-periodic flow $\overline{\psi}_i(\eta)$ must ϵ times as high as that of $\tilde{\psi}_0(r,\chi)$. We thus have

$$\frac{d^4\overline{\psi}_i}{d\eta^4} = -\epsilon\alpha\left[\overline{\frac{\partial(\tilde{\psi}_i,\tilde{\psi}_{i\eta\eta})}{\partial(\eta,\chi)}}\right] = \epsilon\frac{d}{d\eta}M(\eta), \tag{4.10}$$

where

$$M(\eta) = \tfrac{1}{2}i\alpha f(\eta)\frac{d^2}{d\eta^2}f^*(\eta), \tag{4.11}$$

f^* being the complex conjugate of f. The solution is

$$\overline{\psi}_i(\eta) = \epsilon\left[\tfrac{1}{2}\int_0^\eta \eta^2 M\,d\eta - \eta\int_0^\eta \eta M\,d\eta + \tfrac{1}{2}\eta^2\int_\infty^\eta M\,d\eta\right]. \tag{4.12}$$

After matching, the outer solution becomes the vortex

$$\overline{\psi}_0(\eta) = -\epsilon^{\frac{2}{3}}\left(\int_0^\infty \eta M\,d\eta\right)\ln r. \tag{4.13}$$

The uniformly valid solution of the non-periodic flow is then

$$\overline{\psi}(\eta) = -\epsilon^{\frac{2}{3}}\left(\int_0^\infty \eta M\,d\eta\right)\ln r + \epsilon\left[\tfrac{1}{2}\int_0^\eta \eta^2 M\,d\eta + \tfrac{1}{2}\eta^2\int_\infty^\eta M\,d\eta\right] + O(\epsilon^{\frac{4}{3}}). \tag{4.14}$$

λ	Re $H_{\frac{1}{3}}^{(1)}(i^{\frac{1}{2}}\lambda)$	Im $H_{\frac{1}{3}}^{(1)}(i^{\frac{1}{2}}\lambda)$	Re $H_{\frac{2}{3}}^{(1)}(i^{\frac{1}{2}}\lambda)$	Im $H_{\frac{2}{3}}^{(1)}(i^{\frac{1}{2}}\lambda)$
0	$-\infty$	$-\infty$	$-\infty$	$-\infty$
0·2	−0·074507	−1·346130	−0·776625	−1·704071
0·4	0·088990	−0·866273	−0·322633	−1·024403
0·6	0·158068	−0·611439	−0·128633	−0·726528
0·8	0·187598	−0·443076	−0·022740	−0·544138
1·0	0·195821	−0·322020	0·039124	−0·415929
1·2	0·191568	−0·231570	0·075045	−0·319521
1·4	0·179930	−0·162837	0·094408	−0·244494
1·6	0·164122	−0·110362	0·102816	−0·185123
1·8	0·146268	−0·070434	0·103908	−0·137844
2.0	0·127798	−0·040351	0·100183	−0·100207
2·2	0·109671	−0·018050	0·093404	−0·070401
2·4	0·092515	−0·001904	0·084836	−0·047011
2·6	0·076716	0·009392	0·075390	−0·028890
2·8	0·062491	0·016899	0·065712	−0·015090
3·0	0·049926	0·021480	0·056256	−0·004814
3.2	0·039022	0·023840	0·047324	0·002609
3·4	0·029716	0·024549	0·039109	0·007750
3·6	0·021904	0·024068	0·031719	0·011087
3·8	0·015455	0·022766	0·025199	0·013022
4·0	0·010228	0·020932	0·019548	0·013889
4·2	0·006074	0·018791	0·014734	0·013964
4·4	0·002849	0·016514	0·010702	0·013472
4·6	0·000413	0·014229	0·007385	0·012593
4·8	−0·001360	0·012026	0·004708	0·011470
5·0	−0·002592	0·009967	0·002592	0·010217
5·2	−0·003384	0·008091	0·000962	0·008916
5·4	−0·003828	0·006418	−0·000256	0·007632
5·6	−0·004005	0·004957	−0·001130	0·006408
5·8	−0·003980	0·003705	−0·001722	0·005274
6·0	−0·003810	0·002652	−0·002088	0·004248
6·2	−0·003542	0·001783	−0·002275	0·003340
6·4	−0·003212	0·001081	−0·002325	0·002551
6·6	−0·002849	0·000527	−0·002274	0·001879
6·8	−0·002477	0·000102	−0·002151	0·001317
7·0	−0·002111	−0·000212	−0·001980	0·000856
7·2	−0·001763	−0·000434	−0·001780	0·000487
7·4	−0·001443	−0·000581	−0·001568	0·000198
7·6	−0·001153	−0·000667	−0·001353	−0·000020
7·8	−0·000898	−0·000706	−0·001145	−0·000180
8·0	−0·000676	−0·000708	−0·000950	−0·000291
9·0	−0·000025	−0·000454	−0·000247	−0·000389
10·0	0·000129	−0·000169	0·000030	−0·000213
11·0	0·000098	−0·000021	0·000075	−0·000067
12·0	0·000041	0·000022	0·000047	−0·000000
13·0	0·000008	0·000020	0·000017	0·000014
14·0	−0·000003	0·000010	0·000001	0·000010
15·0	−0·000004	0·000002	−0·000002	0·000004
16·0	−0·000002	−0·000000	−0·000002	0·000000
17·0	−0·000000	−0·000000	−0·000001	−0·000000
18·0	0·000000	−0·000000	−0·000000	−0·000000
19·0	0·000000	−0·000000	0·000000	−0·000000
20·0	0·000000	−0·000000	0·000000	−0·000000

TABLE 1

λ	$\mathrm{Re}\int_\lambda^\infty H_{\frac{1}{3}}^{(1)}(i^{\frac{1}{2}}\lambda)\,d\lambda$	$\mathrm{Im}\int_\lambda^\infty H_{\frac{1}{3}}^{(1)}(i^{\frac{1}{2}}\lambda)\,d\lambda$
0	+0·298858	−1·115355
1	+0·276364	−0·106150
2	+0·107304	+0·043830
3	+0·021364	+0·044075
4	−0·005753	+0·020699
5	−0·008051	+0·005297
6	−0·004350	−0·000581
7	−0·001340	−0·001513
8	−0·000012	−0·000938
9	+0·000281	−0·000336
10	+0·000203	−0·000033
11	+0·000083	+0·000050
12	+0·000014	+0·000043
13	−0·000008	+0·000020
14	−0·000009	+0·000004
15	−0·000004	−0·000001
16	−0·000001	−0·000001
17	+0·000000	−0·000001
18	+0·000000	−0·000000
19	+0·000000	−0·000000
20	+0·000000	+0·000000

TABLE 2

The surface shear due to $\tilde{\psi}$ is

$$\tilde{\tau} = -\epsilon^{\frac{2}{3}}\mu\omega e^{i\chi}f''(0) = \epsilon^{\frac{2}{3}}\mu\omega e^{i\chi}2^{\frac{4}{3}}(3\alpha)^{\frac{1}{3}}i^{\frac{2}{3}}/\Gamma(\tfrac{2}{3}). \tag{4.15}$$

The total normal force on the cylinder is thus

$$N = \epsilon\omega^2 a(\mathscr{M}+\mathscr{M}') - \epsilon 2\pi a^3\omega^2\rho + a\int_0^{2\pi}\tilde{\tau}\cos\chi\,d\chi. \tag{4.16}$$

The first term on the right-hand side of (4.16) is the centrifugal force, where $\mathscr{M}$ is the mass of the cylinder and $\mathscr{M}'$ is the virtual mass of the cylinder produced by the rotary translation of the frame of reference. The second term can be identified as the lift due to circulation and the third is the normal force due to viscous shear. Equation (4.16) can be simplified to

$$\frac{N}{\rho\omega^2a^3} = \epsilon\pi\frac{\rho_s}{\rho} - \epsilon\pi + \epsilon^{\frac{5}{3}}\frac{\pi 6^{\frac{1}{3}}}{\alpha^{\frac{2}{3}}\Gamma(\frac{2}{3})} + O(\epsilon^{\frac{7}{3}}), \tag{4.17}$$

where ρ_s is the density of the solid cylinder. The total drag is entirely due to shear stress since the normal pressure of the inviscid outer flow does not contribute to the drag:

$$\frac{D}{\rho\omega^2a^3} = \frac{-1}{\rho\omega^2a^2}\int_0^{2\pi}\tilde{\tau}\sin\chi\,d\chi = \epsilon^{\frac{5}{3}}\pi 2^{\frac{1}{3}}3^{\frac{5}{6}}/\alpha^{\frac{2}{3}}\Gamma(\tfrac{2}{3}) + O(\epsilon^{\frac{7}{3}}). \tag{4.18}$$

The surface shear due to the non-periodic flow is

$$\bar{\tau} = -\mu\epsilon^{\frac{1}{3}}\omega\bar{\psi}_i''(0) = \epsilon^{\frac{4}{3}}\mu\omega 3^{\frac{7}{6}}\alpha^{\frac{2}{3}}\Gamma(\tfrac{2}{3})/2^{\frac{4}{3}}\pi. \tag{4.19}$$

The total torque experienced by the eccentric cylinder is the sum of the torques due to the primary vortex $\ln r$ from (1.11), the non-periodic shear (4.19) and the drag (4.18):

$$T = 2\pi a^2\mu\omega - 2\pi a^2\bar{\tau} + \epsilon a D \tag{4.20}$$

or

$$\frac{T}{2\pi a^2\mu\omega} = 1 - \epsilon^{\frac{4}{3}}\frac{3^{\frac{7}{6}}\alpha^{\frac{2}{3}}\Gamma(\frac{2}{3})}{2^{\frac{4}{3}}\pi} + \epsilon^{\frac{5}{3}}\frac{3^{\frac{5}{6}}\alpha^{\frac{1}{3}}}{2^{\frac{2}{3}}\Gamma(\frac{2}{3})} + O(\epsilon^2)$$

$$= 1 - (\epsilon^2 R^{\frac{2}{3}})\frac{3^{\frac{7}{6}}\Gamma(\frac{2}{3})}{2^{\frac{4}{3}}\pi} + (\epsilon^2 R^{\frac{1}{3}})\frac{3^{\frac{5}{6}}}{2^{\frac{2}{3}}\Gamma(\frac{2}{3})} + O(\epsilon^2). \tag{4.21}$$

5. Low Reynolds numbers $R \ll 1$

For Reynolds numbers lower than order unity there are no boundary layers. From (2.9), the equation

$$-\frac{\partial}{\partial\chi}\nabla^2\tilde{\psi} = \frac{1}{R}\nabla^4\tilde{\psi} \tag{5.1}$$

adequately describes the periodic solution for all r. The solution satisfying boundary conditions (1.13) and (1.14) is

$$\tilde{\psi} = \frac{ie^{i\chi}}{H_0^{(1)}[(iR)^{\frac{1}{2}}]}\left[\frac{2}{(iR)^{\frac{1}{2}}}H_1^{(1)}[(iR)^{\frac{1}{2}}r] - rH_0^{(1)}[(iR)^{\frac{1}{2}}] - \frac{1}{r}H_2^{(1)}[(iR)^{\frac{1}{2}}]\right]. \tag{5.2}$$

The Hankel functions in (5.2) are tabulated in, for example, Jahnke & Emde (1945) and Tölke (1936). Note that even for very small R the left-hand side of (5.1) cannot be neglected. It represents an 'Oseen' correction to the Stokes flow which becomes important at large radii. As R approaches zero we can recover from (5.2) the troublesome $r\ln r$ term which appears in the solution of uniform Stokes flow over a cylinder.

The non-periodic flow caused by nonlinear effects is governed by (3.7). From (3.8)

$$B(r) = -\frac{\epsilon R}{8r}\frac{d}{dr}A, \tag{5.3}$$

$$A = \mathrm{Im}\left(\frac{-2i(iR)^{\frac{1}{2}}}{|H_0^{(1)}[(iR)^{\frac{1}{2}}]|^2}\left[\frac{2}{(iR)^{\frac{1}{2}}}H_1^{(1)}[(iR)^{\frac{1}{2}}r] - rH_0^{(1)}[(iR)^{\frac{1}{2}}] - \frac{1}{r}H_2^{(1)}[(iR)^{\frac{1}{2}}]\right][H_1^{(1)}[(iR)^{\frac{1}{2}}r]]^*\right). \tag{5.4}$$

The streamlines $\bar{\psi}(r)$, which are concentric, can then be calculated from (3.9); their direction depends on the magnitude of R.

The periodic pressure and shear distributions are

$$\frac{\tilde{p}}{\rho\omega^2 a^2\epsilon} = \frac{i}{R}\left(\frac{\partial^3\tilde{\psi}}{\partial r^3} + \frac{\partial^2\tilde{\psi}}{\partial r^2}\right)_{r=1} = 2ie^{i\chi}\left[1 - \frac{H_1^{(1)}[(iR)^{\frac{1}{2}}]}{(iR)^{\frac{1}{2}}H_0^{(1)}[(iR)^{\frac{1}{2}}]}\right], \tag{5.5}$$

$$\frac{\tilde{\tau}}{\mu\omega\epsilon} = -\left.\frac{\partial^2\tilde{\psi}}{\partial r^2}\right|_{r=1} = \frac{2i(iR)^{\frac{1}{2}}H_1^{(1)}[(iR)^{\frac{1}{2}}]}{H_0^{(1)}[(iR)^{\frac{1}{2}}]}e^{i\chi}. \tag{5.6}$$

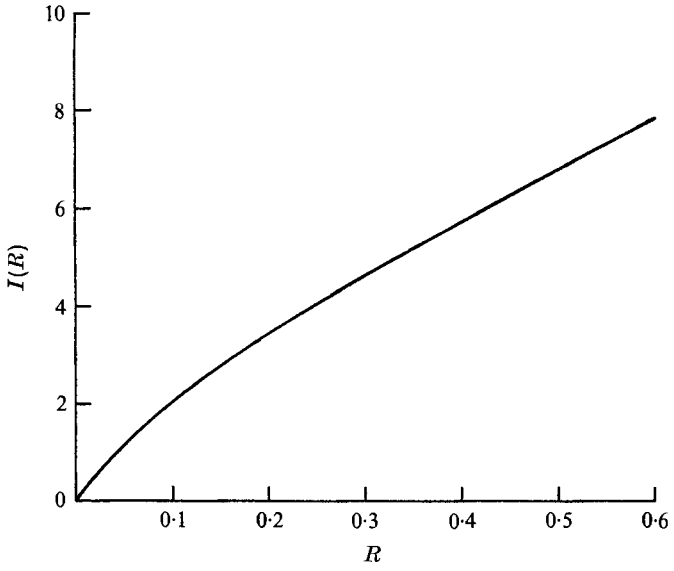

FIGURE 2. The integral $I(R)$, from (5.10).

The total normal force may be obtained by integration:

$$\frac{N}{\rho\omega^2 a^3} = \epsilon\pi\left(1+\frac{\rho_s}{\rho}\right) - \epsilon 2\pi + \frac{1}{\rho\omega^2 a^2}\int_0^{2\pi}(\tilde{\tau}\cos\chi - \tilde{p}\sin\chi)\,d\chi$$

$$= \epsilon\pi\frac{\rho_s}{\rho} - \epsilon\pi + 2\epsilon\pi\left[1 - \frac{2H_1^{(1)}[(iR)^{\frac{1}{2}}]}{(iR)^{\frac{1}{2}}H_0^{(1)}[(iR)^{\frac{1}{2}}]}\right] + O(\epsilon^3), \tag{5.7}$$

where the centrifugal forces and the lift due to circulation have been included. The drag on the cylinder is found to be

$$\frac{D}{\rho\omega^2 a^3} = \frac{1}{\rho\omega^2 a^2}\int_0^{2\pi}(-\tilde{\tau}\sin\chi - \tilde{p}\cos\chi)\,d\chi = \frac{\epsilon 4\pi i H_1^{(1)}[(iR)^{\frac{1}{2}}]}{(iR)^{\frac{1}{2}}H_0^{(1)}[(iR)^{\frac{1}{2}}]} + O(\epsilon^3). \tag{5.8}$$

From (3.9), (5.3) and (5.4) we have

$$\left.\frac{d^2\overline{\psi}}{dr^2}\right|_{r=1} = 4\int_1^\infty Br\ln r\,dr = -\tfrac{1}{2}\epsilon I(R), \tag{5.9}$$

where

$$I(R) = -R\int_1^\infty \frac{A(r,R)}{r}\,dr, \tag{5.10}$$

which cannot be evaluated analytically. Numerical integration gives the results shown in figure 2.

The shear stress due to the non-periodic flow $\overline{\psi}(r)$ is then

$$\overline{\tau} = -\mu\omega\epsilon\overline{\psi}''(1) = \mu\omega\tfrac{1}{2}\epsilon^2 I(R). \tag{5.11}$$

The total torque is the sum

$$T = 2\pi a^2\mu\omega - 2\pi a^2\overline{\tau} + \epsilon a D \tag{5.12}$$

or

$$\frac{T}{2\pi a^2\mu\omega} = 1 - \tfrac{1}{2}\epsilon^2 I(R) + \epsilon^2 2(iR)^{\frac{1}{2}}\frac{H_1^{(1)}[(iR)^{\frac{1}{2}}]}{H_0^{(1)}[(iR)^{\frac{1}{2}}]} + O(\epsilon^4). \tag{5.13}$$

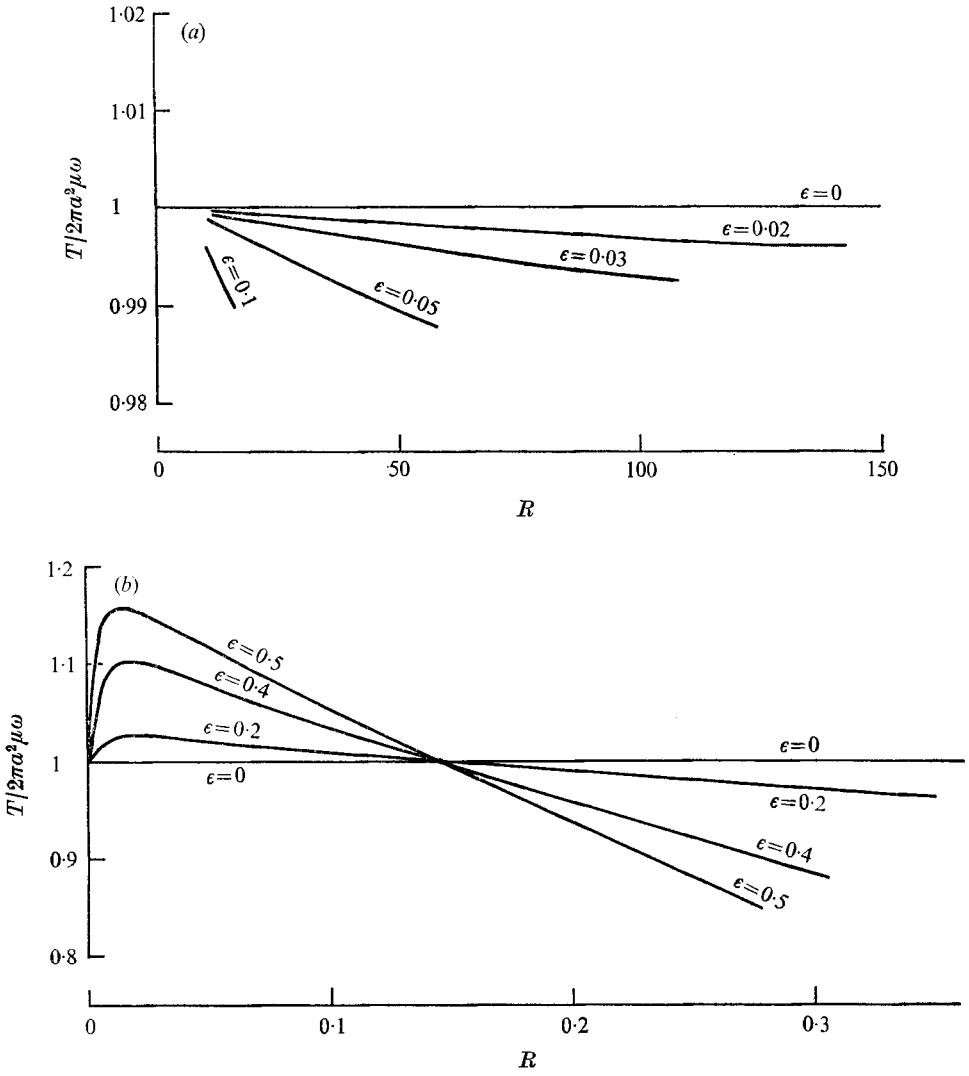

FIGURE 3. Normalized total torque versus Reynolds number at different eccentricities. (*a*) $1 \ll R \ll \epsilon^{-\frac{3}{2}}$. (*b*) $R \ll 1$.

6. Discussion

The most important result is the change in torque due to eccentricity. For high Reynolds numbers, such that $1 \ll R \ll \epsilon^{-\frac{3}{2}}$, the torque is represented by equation (4.21). The first term on the right-hand side represents the torque when eccentricity is absent; the second term is due to the nonlinear Reynolds stress, which causes a *reduction* in torque; the third term, an *increase* in torque, is due to the linear drag on the cylinder. Equation (4.21) is plotted in figure 3 (*a*) for the range of Reynolds numbers considered. The total torque is decreased because of eccentricity.

For low Reynolds numbers the interpretation of the various terms in (5.13) is similar to that of those in (4.21). However, the linear increase in torque is

now comparable with the nonlinear reduction in torque. Figure 3(*b*) shows that the torque is increased when $R < 0{\cdot}145$ and decreased when $R > 0{\cdot}145$, where nonlinear effects become more important. In this figure results for the values $0{\cdot}4$ and $0{\cdot}5$ of ϵ, a parameter supposed much smaller than one, are given for comparison.

It is easy to see why the linear drag, multiplied by the moment arm ea, increases the torque. The nonlinear *decrease* in torque is due to the fact that the Reynolds stress produces a non-periodic streaming in the *same* direction as that of the rotation. The local shear stress, and thus the torque, are then alleviated. Riley (1971) considered a different problem, in which the cylinder is *not* rotating at all but its geometric axis is describing a circular motion. He also concluded that the non-periodic streaming is in the same direction as the circular motion. (Note: in our case the cylinder is rotating with the *same* frequency as the geometric axis.) Physically, the cylinder is performing a periodic scraping motion with respect to the outer fluid. The (nonlinear) mean part is thus in the same direction as the scraping.

Lastly we mention a paper by Wang (1969) in which a rotating cylinder is vibrating laterally along a straight line. The rotation frequency is assumed to be either very large or very small compared with the vibration frequency. Because this is basically an unsteady problem, the time variable cannot be eliminated by a co-ordinate transform as in the present case. The steady streamlines are found by similar matched asymptotic expansions.

REFERENCES

Chang, W. 1948 Der Spannungszustand in Kreisringschale und ähnlichen Schalen mit Scheitelkreisringen unter drehsymmetrischer Belastung. *Nat. Tsing Hwa Sc. Rep.* no. A5, 289–349.

Harvard University Computation Laboratory 1954 *Tables of the Modified Hankel Functions of order One-Third and of their Derivatives.* Harvard University Press.

Jahnke, E. & Emde, F. 1945 *Tables of Functions with Formulae and Curves*, 4th edn. Dover.

Riley, N. 1971 Stirring of viscous fluid. *Z. Angew. Math. Phys.* **22**, 645–653.

Tölke, F. 1936 *Besselsche und Hankelsche Zylinderfunktionen.* Stuttgart: Verlag von Konrad Wittwer.

Wang, C.-Y. 1969 Lateral vibrations of a rotating shaft in a viscous fluid. *J. Appl. Mech.* **36**, 682–686.